arXiv:0705.0290 [astro-ph]

PArthENoPE : Public Algorithm Evaluating the Nucleosynthesis of Primordial Elements

O. Pisanti[1]*, A. Cirillo[1], S. Esposito[1], F. Iocco[1,2], G. Mangano[1], G. Miele[1], and P. D. Serpico[3]
[1] *Dipartimento di Scienze Fisiche, Università di Napoli Federico II and INFN, Sezione di Napoli, Via Cintia, I-80126 Napoli, Italy*
[2] *Kavli Institute for Particle Astrophysics and Cosmology, PO Box 20450, Stanford, CA 94309, USA*
[3] *Center for Particle Astrophysics, Fermi National Accelerator Laboratory, Batavia, IL 60510-0500, USA*

We describe a program for computing the abundances of light elements produced during Big Bang Nucleosynthesis which is publicly available at http://parthenope.na.infn.it/. Starting from nuclear statistical equilibrium conditions the program solves the set of coupled ordinary differential equations, follows the departure from chemical equilibrium of nuclear species, and determines their asymptotic abundances as function of several input cosmological parameters as the baryon density, the number of effective neutrino, the value of cosmological constant and the neutrino chemical potential. The program requires commercial NAG library routines.

Program summary

Title of program: PArthENoPE
Program URL: http://parthenope.na.infn.it/
Program obtainable from: parthenope@na.infn.it
Computers: PC-compatible running Fortran on Unix, MS Windows or Linux
Operating systems under which the program has been tested: Windows 2000, Windows XP, Linux
Programming language used: Fortran 77
External routines/libraries used: NAG libraries
No. of lines in distributed program, including input card and test data: 4969
No. of bytes in distributed program, including input card and test data: 192 Kb
Distribution format: tar.gz
Nature of physical problem: Computation of yields of light elements synthesized in the primordial universe.
Method of solution: BDF method for the integration of the ODE's, implemented in a NAG routine
Typical running time: 90 sec with default parameters on a Dual Xeon Processor 2.4GHz with 2.GB RAM

PACS numbers: 26.35.+c DSF 13/07, FERMILAB-PUB-07-079-A, SLAC-PUB-12488

"A l'alta fantasia qui mancò possa;
ma già volgeva il mio disio e 'l velle,
sì come rota ch'igualmente è mossa,
l'amor che move il sole e l' altre stelle."

Dante Alighieri, "Commedia" - Paradiso, Canto XXXIII, 142-145

I. INTRODUCTION

Big Bang Nucleosynthesis (BBN) is one of the fundamental pillars of the Cosmological Standard Model. In the very early Universe, when the temperature of the primordial plasma decreased from a few MeV down to $\sim 10\,\mathrm{keV}$, light nuclides as ^{2}H, ^{3}He, ^{4}He and, to a smaller extent, ^{7}Li were produced via a network of nuclear processes. The relative abundances of these nuclear "ashes" with respect to hydrogen can be determined via several observational techniques and in different astrophysical environments. In the standard cosmological scenario and in the framework of the electroweak Standard Model, the dynamics of this phase is controlled by only one free parameter, the baryon to photon number density, which can thus be fixed by fitting experimental observations. This parameter can be

* Corresponding author. E-mail: pisanti@na.infn.it

also independently measured with very high precision by Cosmic Microwave Background anisotropies [1] and the agreement with BBN result is quite remarkable. For reviews see e.g. [2] in [3] or [4].

More in general, the quality and quantity of new cosmological and astrophysical data available in the last decade has led to an overall consistent picture of the evolution of the Universe, usually referred to as the "concordance" model. This is based on standard physics plus a few phenomenological parameters, for which an underlying theory is however still missing. At present, one thus faces the intriguing possibility that one might test models which go beyond our present understanding of fundamental interactions, in a way which is complementary to traditional earth-based laboratory and accelerator approaches. This is illustrated e.g. by the search for new light degrees of freedom which might contribute to the total energy density in the Universe in addition to photons and neutrinos. To pursue this programme, it is crucial to achieve a high level of accuracy in theoretical predictions for cosmological observables, at least at the level of experimental uncertainties. In the case of BBN, many steps have been done in this direction by a careful analysis of several key aspects of the physics involved in the phenomenon. The accuracy of the weak reactions which enter the neutron/proton chemical equilibrium has been pushed well below the percent level [5–9]. Similarly, the neutrino decoupling has been carefully studied by several authors by explicitly solving the corresponding kinetic equations [10–15]. These two issues are mainly affecting the prediction of ^{4}He mass fraction, which presently has a very small uncertainty, of the order of 0.1 %, due to the experimental uncertainty on neutron lifetime. Finally, much study has been devoted to the analysis of several nuclear reaction rates entering the BBN network, as well as the corresponding uncertainties. This task involves a careful study of the available data or predictions on each reaction, including an update in light of new relevant experimental measurements, the choice of a reasonable protocol to combine them in order to obtain a best estimate and an error and, finally, the calculation of the corresponding thermal averaged rates. This issue has been extensively discussed in [9], whose results have been used in the program described in the present paper, and [16, 17]. An important benchmark in this development has been represented by the compilation of the NACRE Collaboration database [18].

In view of all these recent developments, we believe that the scientific community interested in BBN, in itself or as a tool to constrain new physics beyond the Standard Model, might find useful a new public BBN code which updates the pioneering achievements of [19–21][1]. For this reason we have publicly released a code we have developed and continuously updated over almost a decade, which we named `PArthENoPE` and can be obtained at the URL http://parthenope.na.infn.it/. The aim of the present paper is to give a general description of the program and how to use it. After briefly summarizing in Section II the theoretical framework of BBN and all major improvements implemented in `PArthENoPE` , we discuss in Section III a few extensions of the minimal standard BBN scenario which are also included in the code. In Section IV the main structures of `PArthENoPE` are outlined, while a comparison with the public code of [20] is discussed in Section V. Finally, in Section VI we report our conclusions. Hereafter we use natural units where the reduced Planck constant, the speed of light and the Boltzmann constant are fixed to 1, i.e. $\hbar = c = k_B = 1$.

II. THE THEORY OF BIG BANG NUCLEOSYNTHESIS

A. The set of equations

We consider N_{nuc} species of nuclides, whose number densities, n_i, are normalized with respect to the total number density of baryons n_B,

$$X_i = \frac{n_i}{n_B} \qquad i = n,\, p,\, ^2\mathrm{H},\, ... \quad . \tag{1}$$

The list of all nuclides which are typically included in BBN analyses and considered in `PArthENoPE` is reported in Table I.

In the (photon) temperature range of interest for BBN, $10\,\mathrm{MeV} > T > 0.01\,\mathrm{MeV}$, electrons and positrons are kept in thermodynamical equilibrium with photons by fast electromagnetic interactions and distributed according to a Fermi-Dirac distribution function $f_{e^\pm}$, with chemical potential μ_e, parameterized in the following by the function $\phi_e \equiv \mu_e/T$. The pressure and energy density of the electromagnetic plasma ($e^\pm$ and γ) is calculated in `PArthENoPE` by including the effect of finite temperature QED corrections [13]. Furthermore, electromagnetic and nuclear scatterings

[1] It is a pleasure to acknowledge the public code of [20] as the starting point for many scholars interested in BBN, including the authors of the present paper.

No.	Nuclide	No.	Nuclide	No.	Nuclide	No.	Nuclide	No.	Nuclide
1	n	7	^{6}Li	13	^{10}B	19	^{13}C	25	^{15}O
2	p	8	^{7}Li	14	^{11}B	20	^{13}N	26	^{16}O
3	^{2}H	9	^{7}Be	15	^{11}C	21	^{14}C		
4	^{3}H	10	^{8}Li	16	^{12}B	22	^{14}N		
5	^{3}He	11	^{8}B	17	^{12}C	23	^{14}O		
6	^{4}He	12	^{9}Be	18	^{12}N	24	^{15}N		

TABLE I: Nuclides considered in `PArthENoPE` .

keep the non-relativistic baryons in kinetic equilibrium, and their energy density ρ_B and pressure p_B are given by

$$\rho_B = \left[M_u + \sum_i \left(\Delta M_i + \frac{3}{2} T \right) X_i \right] n_B \ , \tag{2}$$

$$\mathrm{p}_B = T\, n_B \sum_i X_i \ , \tag{3}$$

with ΔM_i and M_u the i-th nuclide mass excess and the atomic mass unit, respectively.

The set of differential equations ruling primordial nucleosynthesis is the following (see for example [7, 8, 19]):

$$\frac{\dot{a}}{a} = H = \sqrt{\frac{8\,\pi G_N}{3}\ \rho} \quad , \tag{4}$$

$$\frac{\dot{n}_B}{n_B} = -\,3\,H \quad , \tag{5}$$

$$\dot{\rho} = -\,3\,H\ (\rho + \mathrm{p}) \quad , \tag{6}$$

$$\dot{X}_i = \sum_{j,k,l} N_i \left(\Gamma_{kl\to ij}\ \frac{X_l^{N_l}\, X_k^{N_k}}{N_l!\, N_k!} \ - \ \Gamma_{ij\to kl}\ \frac{X_i^{N_i}\, X_j^{N_j}}{N_i!\, N_j!} \right) \equiv \Gamma_i \quad , \tag{7}$$

$$n_B \ \sum_j Z_j\, X_j = n_{e^-} - n_{e^+} \equiv L\left(\frac{m_e}{T}, \phi_e\right) \equiv T^3\ \hat{L}\left(\frac{m_e}{T}, \phi_e\right) \quad , \tag{8}$$

where ρ and p denote the total energy density and pressure, respectively,

$$\rho = \rho_\gamma + \rho_e + \rho_\nu + \rho_B \quad , \tag{9}$$

$$\mathrm{p} = \mathrm{p}_\gamma + \mathrm{p}_e + \mathrm{p}_\nu + \mathrm{p}_B \quad , \tag{10}$$

while i, j, k, l denote nuclear species, N_i the number of nuclides of type i entering a given reaction (and analogously N_j, N_k, N_l), and the Γ's denote symbolically the reaction rates. For example, in the case of decay of the species i, $N_i = 1$, $N_j = 0$ and $\sum \Gamma_{i\to kl}$ is the inverse lifetime of the nucleus i; for binary collisions, $N_i = N_j = N_k = N_l = 1$ and $\Gamma_{ij\to kl} = \langle \sigma_{ij\to kl}\, v \rangle$, i.e. it represents the thermal average of the cross section for the reaction $i + j \to k + l$ times the relative velocity of i and j. In Eq. (8), Z_i is the charge number of the $i-$th nuclide, and the function $\hat{L}(\xi, \omega)$ is defined as

$$\hat{L}(\xi, \omega) \equiv \frac{1}{\pi^2} \int_\xi^\infty d\zeta\ \zeta\ \sqrt{\zeta^2 - \xi^2}\ \left(\frac{1}{e^{\zeta - \omega} + 1} - \frac{1}{e^{\zeta + \omega} + 1} \right) \quad . \tag{11}$$

Equation (4) is the definition of the Hubble parameter H, a denoting the scale factor of the Friedmann-Robertson-Walker-Lemaître metric, with G_N the gravitational constant, whereas Eq.s (5) and (6) state the total baryon number and entropy conservation per comoving volume, respectively. The set of N_{nuc} Boltzmann equations (7) describes the density evolution of each nuclide specie, with $\Gamma_{kl\to ij}$ the rate per incoming particles averaged over kinetic equilibrium distribution functions. Finally, Eq. (8) states the Universe charge neutrality in terms of the electron chemical potential, with $L\,(m_e/T, \phi_e)$ the charge density in the lepton sector in unit of the electron charge.

The neutrino energy density and pressure are defined in terms of their distributions in momentum space as

$$\rho_\nu = 3\,\mathrm{p}_\nu = 2 \int \frac{d^3p}{(2\pi)^3}\ |\vec{p}|\ [f_{\nu_e} + 2\, f_{\nu_x}] \quad , \tag{12}$$

Indeed, in the default scenario we assume a vanishing neutrino chemical potential, so that $f_{\nu_e} = f_{\bar{\nu}_e}$ and $f_{\nu_x} \equiv f_{\nu_\mu} = f_{\bar{\nu}_\mu} = f_{\nu_\tau} = f_{\bar{\nu}_\tau}$. The nuclide evolution can be followed in `PArthENoPE` also for finite neutrino chemical potential, see Section III below.

As well known, neutrinos decouple from the electromagnetic plasma at temperatures of a few MeV. Soon after, when the onset of $e^+ - e^-$ annihilations takes place, $e^\pm$ are still partially coupled to neutrinos. The neutrino distributions are thus slightly distorted, especially in their high energy tail (and the $e-$flavor more than the other two, since the former also interacts via charged current). To get BBN predictions accurate at the sub-percent level it is necessary to follow in details this residual out of equilibrium neutrino heating by solving the kinetic equations for neutrino distributions. Remarkably, baryons provide a negligible contribution to the dynamics of the Universe at the BBN epoch as the baryon to photon number density is very small, $\eta \lesssim 10^{-9}$, and therefore Boltzmann equations for neutrino species can be solved together with equations (4) and (6) only, ignoring the dynamics of nuclear species. This allows one to solve the evolution of the neutrino species first, and then to substitute the resulting neutrino distribution into the remaining equations. We do not consider neutrino oscillations, whose effect has been studied and shown to be sub-leading in [14]. The reader can find further details on the neutrino decoupling stage in [9, 14, 15].

B. Numerical solution of the BBN set of equations

The BBN set of equations (4)-(8) can be recast in a form more convenient for a numerical solution, which follows the evolution of the $N_{nuc}+1$ unknown quantities $(\phi_e,\ X_j)$ as functions of the dimensionless variable $z = m_e/T$. In this framework, Eq. (8) provides n_B as a function of ϕ_e. In particular, the set of differential equations implemented in `PArthENoPE` is the following:

$$\frac{d\phi_e}{dz} = \frac{1}{z}\frac{\hat{L}\,\kappa_1 + \left(\hat{\rho}_{e\gamma B} + \hat{\mathrm{p}}_{e\gamma B} + \frac{\mathcal{N}(z)}{3}\right)\kappa_2}{\hat{L}\,\frac{\partial\hat{\rho}_e}{\partial\phi_e} - \frac{\partial\hat{L}}{\partial\phi_e}\left(\hat{\rho}_{e\gamma B} + \hat{\mathrm{p}}_{e\gamma B} + \frac{\mathcal{N}(z)}{3}\right)}\ , \tag{13}$$

$$\frac{dX_i}{dz} = \dot{X}_i\frac{dt}{dz} = -\frac{\widehat{\Gamma}_i}{3z\,\widehat{H}}\,\frac{\kappa_1\,\frac{\partial\hat{L}}{\partial\phi_e} + \kappa_2\,\frac{\partial\hat{\rho}_{e\gamma B}}{\partial\phi_e}}{\hat{L}\,\frac{\partial\hat{\rho}_e}{\partial\phi_e} - \frac{\partial\hat{L}}{\partial\phi_e}\left(\hat{\rho}_{e\gamma B} + \hat{\mathrm{p}}_{e\gamma B} + \frac{\mathcal{N}(z)}{3}\right)}\ , \tag{14}$$

where

$$\kappa_1 = 4\,(\hat{\rho}_e + \hat{\rho}_\gamma) + \frac{3}{2}\,\hat{\mathrm{p}}_B - z\,\frac{\partial\hat{\rho}_e}{\partial z} - z\,\frac{\partial\hat{\rho}_\gamma}{\partial z} + \frac{1}{\hat{L}}\left(3\,\hat{L} - z\frac{\partial\hat{L}}{\partial z}\right)\hat{\rho}_B - \frac{z^2\,\hat{L}}{\sum_j Z_j\,X_j}\sum_i\left(\Delta\widehat{M}_i + \frac{3}{2\,z}\right)\widehat{\Gamma}_i\ , \tag{15}$$

$$\kappa_2 = z\,\frac{\partial\hat{L}}{\partial z} - 3\,\hat{L} - z\,\hat{L}\,\frac{\sum_i Z_i\,\widehat{\Gamma}_i}{\sum_j Z_j\,X_j}\ . \tag{16}$$

See Appendix A for notations and the explicit derivation of this set of equations. Equations (13) and (14) are solved by imposing the following initial conditions at $z_{in} = m_e/(10\,\mathrm{MeV})$:

$$\phi_e(z_{in}) = {\phi_e}^0\ , \tag{17}$$

$$X_1(z_{in}) \equiv X_n(z_{in}) = (\exp\{\hat{q}\,z_{in}\}+1)^{-1}\ , \tag{18}$$

$$X_2(z_{in}) \equiv X_p(z_{in}) = (\exp\{-\hat{q}\,z_{in}\}+1)^{-1}\ , \tag{19}$$

$$X_i(z_{in}) = \frac{g_i}{2}\left(\zeta(3)\sqrt{\frac{8}{\pi}}\right)^{A_i-1} A_i^{\frac{3}{2}}\left(\frac{m_e}{M_N z_{in}}\right)^{\frac{3}{2}(A_i-1)} \eta_i^{A_i-1}\,X_p^{Z_i}(z_{in}) \times\ X_n^{A_i-Z_i}(z_{in})\,\exp\left\{\hat{B}_i\,z_{in}\right\} \qquad i = {}^2\mathrm{H},\,{}^3\mathrm{H},\ldots\ . \tag{20}$$

In the previous equations $\hat{q} = (M_n - M_p)/m_e$, and the quantities A_i and $\hat{B}_i$ denote the atomic number and the binding energy of the $i-$th nuclide normalized to electron mass, respectively. Also note that Eq. (20) is only applied if the

No.	Reaction	Type	No.	Reaction	Type
1	$n \leftrightarrow p$	*weak*	22	$^6Li + p \leftrightarrow \gamma + {}^7Be$	(p,γ)
2	$^3H \rightarrow \bar{\nu}_e + e^- + {}^3He$	*weak*	23	$^6Li + p \leftrightarrow {}^3He + {}^4He$	^{3}He Pickup
3	$^8Li \rightarrow \bar{\nu}_e + e^- + 2\ {}^4He$	*weak*	24	$^7Li + p \leftrightarrow {}^4He + {}^4He$	^{4}He Pickup
4	$^{12}B \rightarrow \bar{\nu}_e + e^- + {}^{12}C$	*weak*	24 bis	$^7Li + p \leftrightarrow \gamma + {}^4He + {}^4He$	(p,γ)
5	$^{14}C \rightarrow \bar{\nu}_e + e^- + {}^{14}N$	*weak*	25	$^4He + {}^2H \leftrightarrow \gamma + {}^6Li$	(d,γ)
6	$^8B \rightarrow \nu_e + e^+ + 2\ {}^4He$	*weak*	26	$^4He + {}^3H \leftrightarrow \gamma + {}^7Li$	(t,γ)
7	$^{11}C \rightarrow \nu_e + e^+ + {}^{11}B$	*weak*	27	$^4He + {}^3He \leftrightarrow \gamma + {}^7Be$	(^{3}He,γ)
8	$^{12}N \rightarrow \nu_e + e^+ + {}^{12}C$	*weak*	28	$^2H + {}^2H \leftrightarrow n + {}^3He$	^{2}H Strip.
9	$^{13}N \rightarrow \nu_e + e^+ + {}^{13}C$	*weak*	29	$^2H + {}^2H \leftrightarrow p + {}^3H$	^{2}H Strip.
10	$^{14}O \rightarrow \nu_e + e^+ + {}^{14}N$	*weak*	30	$^3H + {}^2H \leftrightarrow n + {}^4He$	^{2}H Strip.
11	$^{15}O \rightarrow \nu_e + e^+ + {}^{15}N$	*weak*	31	$^3He + {}^2H \leftrightarrow p + {}^4He$	^{2}H Strip.
12	$p + n \leftrightarrow \gamma + {}^2H$	(n,γ)	32	$^3He + {}^3He \leftrightarrow p + p + {}^4He$	(^{3}He,2p)
13	$^2H + n \leftrightarrow \gamma + {}^3H$	(n,γ)	33	$^7Li + {}^2H \leftrightarrow n + {}^4He + {}^4He$	(d,n α)
14	$^3He + n \leftrightarrow \gamma + {}^4He$	(n,γ)	34	$^7Be + {}^2H \leftrightarrow p + {}^4He + {}^4He$	(d,p α)
15	$^6Li + n \leftrightarrow \gamma + {}^7Li$	(n,γ)	35	$^3He + {}^3H \leftrightarrow \gamma + {}^6Li$	(t,γ)
16	$^3He + n \leftrightarrow p + {}^3H$	charge ex.	36	$^6Li + {}^2H \leftrightarrow n + {}^7Be$	^{2}H Strip.
17	$^7Be + n \leftrightarrow p + {}^7Li$	charge ex.	37	$^6Li + {}^2H \leftrightarrow p + {}^7Li$	^{2}H Strip.
18	$^6Li + n \leftrightarrow {}^3H + {}^4He$	^{3}H Pickup	38	$^3He + {}^3H \leftrightarrow {}^2H + {}^4He$	(^{3}H,d)
19	$^7Be + n \leftrightarrow {}^4He + {}^4He$	^{4}He Pickup	39	$^3H + {}^3H \leftrightarrow n + n + {}^4He$	(t,n n)
20	$^2H + p \leftrightarrow \gamma + {}^3He$	(p,γ)	40	$^3He + {}^3H \leftrightarrow p + n + {}^4He$	(t,n p)
21	$^3H + p \leftrightarrow \gamma + {}^4He$	(p,γ)			

TABLE II: The reactions used in the small network.

resulting abundance is greater than the numerical zero assumed (variable YMIN, whose default setting is 10^{-30}). Finally, η_i is the initial value of the baryon to photon number density ratio at $T = 10\,\mathrm{MeV}$ (for a discussion of how it is related to the final value after $e^+ - e^-$ annihilation stage see e.g. Section 4.2.2 in [9]), and ${\phi_e}^0$ the solution of the implicit equation

$$\hat{L}(z_{in},\, {\phi_e}^0) = \frac{2\,\zeta(3)}{\pi^2}\ \eta_i\ \sum_i Z_i\, X_i(z_{in}) \quad . \tag{21}$$

C. The Nuclear Chain

In Tables II, III, and IV are reported the nuclear processes considered in `PArthENoPE` . The enumeration shown in the first column of the tables correspond to the order in which they appear in the program. See [9] for the relevant formalism concerning the thermally averaged nuclear rates and an analysis of the main experimental reaction rates. Reactions included in Table II are used when running `PArthENoPE` in its simpler version (small network), while those of Tables III and IV are added in the intermediate and complete network running options, which also follows the evolution of the nuclides heavier than ^{7}Be and ^{12}N, respectively. Using the small network gives values of the lighter nuclides like ^{2}H, ^{3}He, ^{4}He and ^{7}Li which differ from the results obtained with the complete network for less than 0.02%, for default values of the input cosmological parameters. With respect to the database used in [9], there are a few minor upgrades implemented here, namely the three reactions (98, 99, 100) have been inserted following the analysis of the extended network reported in [22]. Also, we have added the recent data reported in [23] to the regressions for the rates (28, 29), with results in good agreement with those adopted in [9].

III. NON-STANDARD PHYSICS

In the standard scenario the only free parameter entering the BBN dynamics is the value of the baryon to photon number density η, or equivalently the baryon energy density parameter $\Omega_B h^2$, see e.g. [9] for the relation between these parameters. If one goes beyond the standard framework, the BBN predictions may be altered by non-standard

No.	Reaction	Type	No.	Reaction	Type
41	^{7}Li + ^{3}H ↔ n + ^{9}Be	^{3}H Strip.	58	^{6}Li + ^{4}He ↔ γ + ^{10}B	(α,γ)
42	^{7}Be + ^{3}H ↔ p + ^{9}Be	^{3}H Strip.	59	^{7}Li + ^{4}He ↔ γ + ^{11}B	(α,γ)
43	^{7}Li + ^{3}He ↔ p + ^{9}Be	^{3}He Strip.	60	^{7}Be + ^{4}He ↔ γ + ^{11}C	(α,γ)
44	^{7}Li + n ↔ γ + ^{8}Li	(n,γ)	61	^{8}B + ^{4}He ↔ p + ^{11}C	(α,p)
45	^{10}B + n ↔ γ + ^{11}B	(n,γ)	62	^{8}Li + ^{4}He ↔ n + ^{11}B	(α,n)
46	^{11}B + n ↔ γ + ^{12}B	(n,γ)	63	^{9}Be + ^{4}He ↔ n + ^{12}C	(α,n)
47	^{11}C + n ↔ p + ^{11}B	(n,p)	64	^{9}Be + ^{2}H ↔ n + ^{10}B	(^{2}H,n)
48	^{10}B + n ↔ ^{4}He + ^{7}Li	(n,α)	65	^{10}B + ^{2}H ↔ p + ^{11}B	(^{2}H,p)
49	^{7}Be + p ↔ γ + ^{8}B	(p,γ)	66	^{11}B + ^{2}H ↔ n + ^{12}C	(^{2}H,n)
50	^{9}Be + p ↔ γ + ^{10}B	(p,γ)	67	^{4}He + ^{4}He + n ↔ γ + ^{9}Be	(α n,γ)
51	^{10}B + p ↔ γ + ^{11}C	(p,γ)	68	^{4}He + ^{4}He + ^{4}He ↔ γ + ^{12}C	(α α,γ)
52	^{11}B + p ↔ γ + ^{12}C	(p,γ)	69	^{8}Li + p ↔ n + ^{4}He + ^{4}He	(p,n α)
53	^{11}C + p ↔ γ + ^{12}N	(p,γ)	70	^{8}B + n ↔ p + ^{4}He + ^{4}He	(n,p α)
54	^{12}B + p ↔ n + ^{12}C	(p,n)	71	^{9}Be + p ↔ ^{2}H + ^{4}He + ^{4}He	(p,d α)
55	^{9}Be + p ↔ ^{4}He + ^{6}Li	(p,α)	72	^{11}B + p ↔ ^{4}He + ^{4}He + ^{4}He	(p,α α)
56	^{10}B + p ↔ ^{4}He + ^{7}Be	(p,α)	73	^{11}C + n ↔ ^{4}He + ^{4}He + ^{4}He	(n,α α)
57	^{12}B + p ↔ ^{4}He + ^{9}Be	(p,α)			

TABLE III: The reactions used in the intermediate network in addition to those of Table II.

physics entering e.g. the neutrino [14, 15, 24, 25] or gravity sector [26, 27], or more generically by the presence in the plasma of other degrees of freedom besides the Standard Model ones [28–34]. For an earlier review, see [35]. Typically, constraints on non-minimal and/or exotic scenarios require model-dependent modifications of the equations ruling BBN. In `PArthENoPE` we implement a few of them described below which are general enough to be commonly used/referred to in the specialized literature.

No.	Reaction	Type	No.	Reaction	Type
74	^{12}C + n ↔ γ + ^{13}C	(n,γ)	88	^{12}C + ^{4}He ↔ γ + ^{16}O	(α,γ)
75	^{13}C + n ↔ γ + ^{14}C	(n,γ)	89	^{10}B + ^{4}He ↔ p + ^{13}C	(α,p)
76	^{14}N + n ↔ γ + ^{15}N	(n,γ)	90	^{11}B + ^{4}He ↔ p + ^{14}C	(α,p)
77	^{13}N + n ↔ p + ^{13}C	(n,p)	91	^{11}C + ^{4}He ↔ p + ^{14}N	(α,p)
78	^{14}N + n ↔ p + ^{14}C	(n,p)	92	^{12}N + ^{4}He ↔ p + ^{15}O	(α,p)
79	^{15}O + n ↔ p + ^{15}N	(n,p)	93	^{13}N + ^{4}He ↔ p + ^{16}O	(α,p)
80	^{15}O + n ↔ ^{4}He + ^{12}C	(n,α)	94	^{10}B + ^{4}He ↔ n + ^{13}N	(α,n)
81	^{12}C + p ↔ γ + ^{13}N	(p,γ)	95	^{11}B + ^{4}He ↔ n + ^{14}N	(α,n)
82	^{13}C + p ↔ γ + ^{14}N	(p,γ)	96	^{12}B + ^{4}He ↔ n + ^{15}N	(α,n)
83	^{14}C + p ↔ γ + ^{15}N	(p,γ)	97	^{13}C + ^{4}He ↔ n + ^{16}O	(α,n)
84	^{13}N + p ↔ γ + ^{14}O	(p,γ)	98	^{11}B + ^{2}H ↔ p + ^{12}B	^{2}H Strip.
85	^{14}N + p ↔ γ + ^{15}O	(p,γ)	99	^{12}C + ^{2}H ↔ p + ^{13}C	^{2}H Strip.
86	^{15}N + p ↔ γ + ^{16}O	(p,γ)	100	^{13}C + ^{2}H ↔ p + ^{14}C	^{2}H Strip.
87	^{15}N + p ↔ ^{4}He + ^{12}C	(p,α)			

TABLE IV: The reactions used in the complete network in addition to those of Tables II and III.

A. Energy density of the vacuum, ρ_Λ

As in the original Kawano code [20], we allow for a non-zero cosmological constant term at the BBN epoch. We parameterize it by means of ρ_Λ entering the equations only via

$$3H \to 3\,H = \sqrt{24\,\pi\,G_N\left[\left(\frac{m_e}{z}\right)^4\hat{\rho} + \rho_\Lambda\right]}\,. \tag{22}$$

The allowed range for this parameter in units of MeV^4 is $0 \leq (\rho_\Lambda/\mathrm{MeV}^4) \leq 1$.

B. Extra degrees of freedom, $\Delta N_{\rm eff}$

We parameterize the radiation density in non-electromagnetically interacting particles at the BBN epoch by an additional radiation energy density ρ_X entering H. This is related to the "number of extra effective neutrino species" customarily used in the literature $\Delta N_{\rm eff}$ by the equation

$$\rho_X = \frac{7}{8}\frac{\pi^2}{30}\Delta N_{\rm eff} T_X^4\,, \tag{23}$$

where, from the entropy conservation, $T_X = T = m_e/z$ at temperatures higher than the effective neutrino decoupling temperature, chosen as $T_d = 2.3$ MeV, or else

$$T_X = T\left[\frac{\hat{\rho}_{e,\gamma,B}(T) + \hat{\mathrm{p}}_{e,\gamma,B}(T)}{\hat{\rho}_{e,\gamma,B}(T_d) + \hat{\mathrm{p}}_{e,\gamma,B}(T_d)}\right]^{1/3}\,,\ T < T_d\,. \tag{24}$$

The user may input a value of $\Delta N_{\rm eff}$ in the range $-3.0 \leq \Delta N_{\rm eff} \leq 15.0$.

C. Chemical potential of the neutrinos, ξ

The usual argument in favor of a cosmic lepton asymmetry is that sphaleron effects before electroweak symmetry breaking equilibrate the lepton and baryon asymmetries to within a factor of order unity, thus producing the observed baryon density. In principle, however, the electron-neutrino degeneracy parameter $\xi = \mu_{\nu_e}/T_{\nu_e}$ as well as the degeneracy parameters of the other neutrino flavors are not determined within the Standard Model, and should be constrained observationally. Recently, it has been realized that the measured neutrino oscillation parameters imply that neutrinos reach approximate chemical equilibrium before the BBN epoch. Thus, all neutrino chemical potentials can be taken to be equal, i.e. they are all characterized by the same degeneracy parameter ξ that applies to ν_e [36–38]. In light of these results it is meaningful to assume a single and shared value ξ as the only free input parameter. Also, to achieve an approximate agreement between the observed and predicted light element abundances a possible lepton asymmetry must be small, $|\xi| \ll 1$. For such small ξ values the most important impact on BBN is a shift of the beta equilibrium between protons and neutrons. A subleading effect is a modification of the radiation density,

$$\Delta N_{\rm eff}(\xi) = 3\left[\frac{30}{7}\left(\frac{\xi}{\pi}\right)^2 + \frac{15}{7}\left(\frac{\xi}{\pi}\right)^4\right]. \tag{25}$$

Moreover, the neutrino decoupling temperature is higher than in the standard case [39, 40], so that in principle one could get a non-standard $T_\nu(T)$ evolution, but such effects are completely negligible for our case. A non-zero ξ slightly modifies the partial neutrino reheating following the e^+e^- annihilation [41], again a completely negligible effect for the range of ξ of our interest. In the code, we allow the user to select among 21 possible values of ξ, between -1.0 and +1.0, spaced by 0.1. The changes in the weak reactions are then automatically implemented, as in [8]. The associated change in $\Delta N_{\rm eff}$ of Eq. (25) is also accounted for. Note that to derive results on a finer grid a perturbative approach as the one in [31] would be required. This possibility is left for an implementation in a future upgraded version of the code.

IV. THE STRUCTURE OF `PARTHENOPE`

The code is divided in two files, `main.f` and `parthenope.f`, the former one containing the main program and the latter the remaining subroutines. While all the physics is implemented in `parthenope.f`, the file `main.f` is an interface

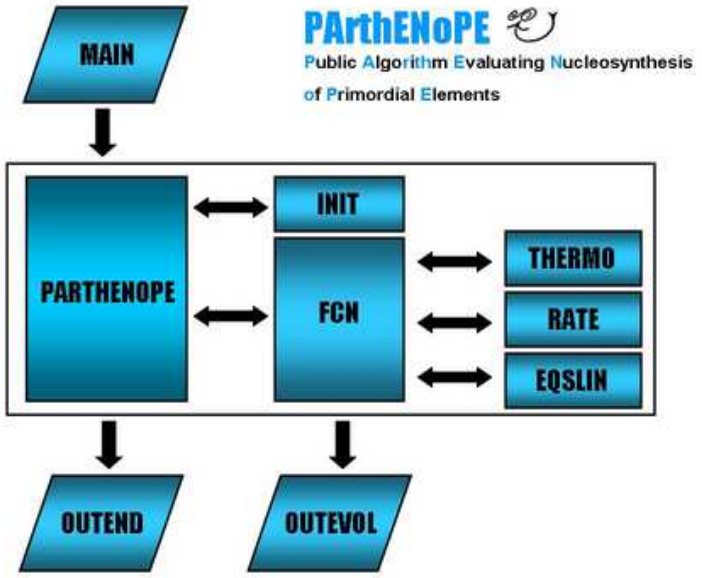

FIG. 1: The logical structure of `PArthENoPE` .

which can be possibly adapted to the user needs. The user can choose between two running modes: an interactive one, with parameter selections given on the screen, and a card mode requiring an input card, an example of which is provided as the file `input` (see also Table VI). The program links to the NAG libraries [42] for some algebraic operations and the evaluation of special functions.

The logical structure of the code is depicted in Figure 1. In the following we detail the aim of each block.

A. `MAIN`

MAIN contains the interface which allows the user to choose the physical and network input parameters and to customize the output.

Physical parameters presently are: baryon density, number of additional neutrino species, neutron lifetime, neutrino chemical potential, energy density of the vacuum at the BBN epoch.

KEYWORD	DESCRIPTION	DEFAULT	RANGE/OPTIONS
OMEGABH	Baryon density $\Omega_B h^2$	0.0223	0.01 ÷ 0.03
DNNU	Number of additional neutrino species	0.	-3. ÷ 15.
TAU	Neutron lifetime	885.7 s	880. ÷ 890.
IXIE	Integer fixing the electron neutrino chemical potential	11	1 ÷ 21
RHOLMBD	Energy density of the vacuum, ρ_Λ, in MeV^4	0.	0. ÷ 1.
NETWORK	Number of nuclides in the network	9	9,18,26
FOLLOW	Option for following the evolution on the screen	F	T,F
OVERWRITE	Option for overwriting the output files	F	T,F
FILES	Name of the output files	parthenope.out	20 bit string
		nuclides.out	20 bit string
OUTPUT	Evolution of nuclides	first 9 nuclides	see text
RATES	Details on changed rates	No change	see text
EXIT	Closing keyword in the input card		

TABLE V: The list of the possible keywords in the input card, their default values and corresponding ranges/options.

RATES	3 (12 1 0.) (28 3 .4) (29 2 0)	options for changing the nuclear rates
RATES	2 (3 2 0.) (5 3 .6)	options for changing the nuclear rates
TAU	885.7	experimental value of neutron lifetime
DNNU	.0	number of extra neutrinos
IXIE	11	integer giving the value of ν_e chemical potential
RHOLMBD	.0	value of cosmological constant energy density at the BBN epoch
OVERWRITE	T	option for overwriting the output files
FOLLOW	T	option for following the evolution on the screen
OMEGABH	.0223	value of $\Omega_B h^2$
NETWORK	9	number of nuclides in the network
FILES	parthenope1.out nuclides1.out	names of the two output files
OUTPUT	T 3 2 3 4	options for customizing the output
EXIT		terminates input

TABLE VI: An example of input card.

Network parameters include: the choice among a small (9 nuclides and 40 reactions), an intermediate (18 nuclides and 73 reactions), and a complete network (26 nuclides and 100 reactions). Moreover, the user can change the rates of each reaction included in the chosen network, selecting a 'LOW' or a 'HIGH' value, based on the experimental or theoretical uncertainties, or a customized multiplicative 'FACTOR'.

Finally, the output options include: the choice of the nuclides whose evolution has to be followed versus z, the name of the output files (a first one with the final results and a second with the evolution of the selected nuclides), and the possibility to follow the status of the evolution on the screen.

All this information can be provided either interactively, following the on-screen instructions, or by an input card, with the format of the example card included in the distribution. In particular, each line in this card must start with an allowed key and the last line key has to be 'EXIT'. In order to be recognized, each key must start at the first bit of the line. The allowed keywords are listed in Table V, together with the default values adopted by the code whenever the corresponding key is not explicitly set.

An example of input card is shown in Table VI. While the keys OMEGABH, DNNU, TAU, IXIE, RHOLMBD, NETWORK, FOLLOW, and OVERWRITE have only one argument, the keyword FILES has two arguments, that is the two names of the output files, each one at most 20 bits long. Some more details deserve the two keywords OUTPUT and RATES. OUTPUT can have at most $N_{nuc} + 2$ arguments (N_{nuc} being the number of nuclides of the chosen network), which are: 1) a bit equal to 'T' or 'F', if the user wants or not to store in the output the evolution of a given set of nuclide abundances, 2) the total number of such nuclides, and 3) the identity of these nuclides (given as the corresponding number in Table I). In the example of Table VI with the sequence T 3 2 3 4 the user has chosen to store in the output the three nuclides p, ^{2}H and ^{3}H. The keyword RATES allows to change the default values of the nuclear rates used in the chosen network. The input card can have more than one line with this keyword, as in the example of Table VI. Each line contains: 1) an integer k, giving the number of reactions whose change is specified on that line; 2) the kind of change for the k reactions with the syntax `(m i f)`, indicating that the reaction number `m` (see Tables II, III and IV) has to be changed according to the type of change `i`, with the factor `f`. Obviously, `m` can assume the values 1,...,M (M being the number of reactions of the chosen network), while `i`=1,2,3 corresponds to the 'LOW', 'HIGH', or 'FACTOR' type of change, respectively. Whenever a statistically sound analysis is possible, as it is the case for most of the main reactions, the 'LOW'/'HIGH' rates represent 1 σ lower/upper limits to the rate, as compiled in [9]. For most of the subleading reactions, they represent estimated ranges of variability, obtained from the literature. The main (or unique) reference from which the rate has been taken is reported as a comment in the code next to the related reaction line. Finally, if `i`=3 the real number `f` is the value of the multiplicative factor applied to the chosen reaction rate (not considered if the options `i`=1,2 are selected). For example, the first line of the input card of Table VI specifies that 3 reaction rates should be changed in running `PArthENoPE` as follows

$$\begin{aligned} \mathrm{p} + \mathrm{n} &\leftrightarrow \gamma + {}^2\mathrm{H} && \text{low rate} \\ {}^2\mathrm{H} + {}^2\mathrm{H} &\leftrightarrow \mathrm{n} + {}^3\mathrm{He} && \text{rate multiplied by the factor 0.4} \\ {}^2\mathrm{H} + {}^2\mathrm{H} &\leftrightarrow \mathrm{p} + {}^3\mathrm{H} && \text{high rate} \end{aligned}$$

Notice that it is possible to add comments after the parameters in the input card and the order of the lines with different keywords is not important.

B. PARTHENOPE

This subroutine drives the resolution of the BBN set of equations. It starts calling the initialization routine INIT, then the NAG solver, finally the output printing routine OUTEND. The NAG resolution parameters, controlling for example the resolution method and the numerical accuracy, have been chosen to optimize the performances of the NAG solver. Any change of these parameters should be implemented only after a careful reading of the NAG manual [42].

Further relevant parameters are `zin` and `zend`, setting respectively the initial and final value of the independent variable z. Their present values correspond to the two temperatures of $T_i = 10\,\mathrm{MeV}$ and $T_f = 1/130\,\mathrm{MeV}$. Note that a few settings depend on these values, which then should be varied with caution.

C. INIT

Besides initializing the nuclear parameters, this subroutine calculates the initial values for all nuclide abundances and the electron chemical potential, the latter requiring the inversion of the implicit equation (21) with a NAG routine.

D. FCN, THERMO, RATE, EQSLIN

The subroutine `FCN` is required by the NAG solver to calculate the right hand side of the differential BBN equations. In order to do this, the thermodynamical quantities which appear in the equations are evaluated with a call to the subroutine `THERMO`. The second step is the calculation of the reaction rates with the subroutine `RATE`. Then the linearization of the set of equations is performed, with the construction of a corresponding $N_{nuc} \times N_{nuc}$ matrix (N_{nuc} being the number of nuclides). In this way, the unknown functions appear in a linear equation system, solved by Gaussian elimination in the subroutine `EQSLIN` (this method is very similar to the one applied in the Kawano code [20]).

E. OUTEVOL, OUTEND

The subroutine `OUTEVOL` is called during the evolution, for printing the intermediate values of the chosen nuclide abundances in one of the output files. Moreover, if requested by the user, this subroutine allows to follow the resolution evolution, printing some physical quantities on the screen. Finally, `OUTEND` prints the final values of the nuclide abundances and electron chemical potential in the other output file along with some technical information on the differential evolution resolution. The final yield of the $i-$th nuclide is expressed as the ratio X_i/X_p, i.e. number density normalized to hydrogen. The only exceptions are Hydrogen expressed as X_p and ^{4}He, which is conventionally reported in terms of the (approximate) mass fraction $Y_p = 4X_{^4\mathrm{He}}$.

V. MAIN DIFFERENCES WITH RESPECT TO THE WAGONER-KAWANO CODE

As we have previously emphasized, the public Kawano code [20] was the starting point for the development of `PArthENoPE` . So, they have a similar structure, like the subdivision in several subroutines which contain, for example, the interface with the user, the calculation of nuclear rates, of the thermodynamical quantities, the differential equation solver, and the production of the output. Here we summarize the main physical and numerical differences with respect to the original code:

- The interface menu and the options are now different. In particular, the user can more easily implement changes in the nuclear reaction network. A card-mode input is available. The output is easily customized.
- Several numerical routines have been replaced with more efficient algorithms, most of which using NAG routines.
- Improved calculations for the $n - p$ reactions are implemented via new fits, not as effective corrections added a posteriori. They also include effects of finite nucleon mass and non-thermal neutrino spectral distortions. The same holds for the case with neutrino asymmetry.

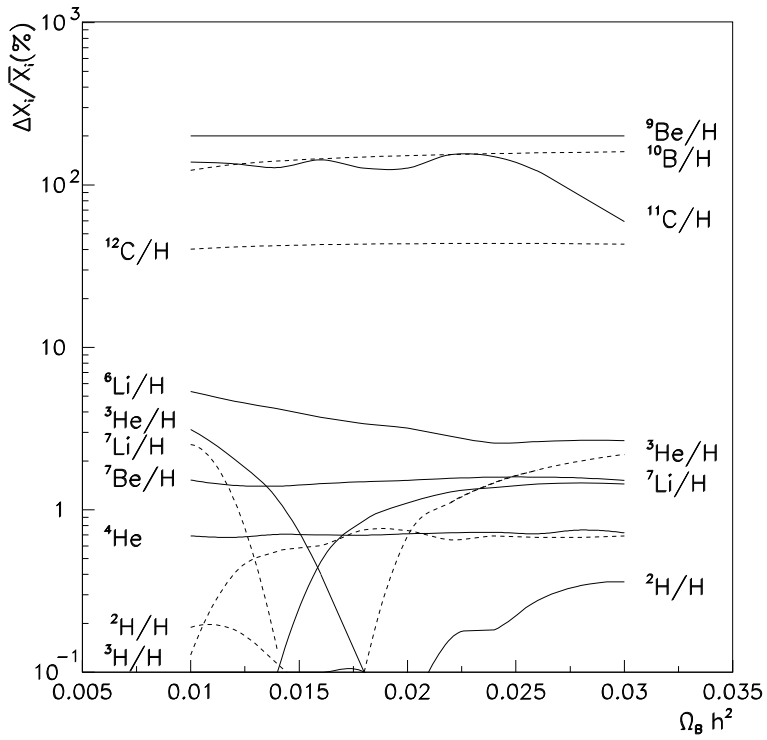

FIG. 2: The relative difference in percent of nuclei abundances between `PArthENoPE` and the Kawano code, $\Delta X_i/\bar{X}_i \equiv 2(X_i^P - X_i^K)/(X_i^P + X_i^K)$, versus baryon density $\Omega_B h^2$. The solid (dashed) curves are for positive (negative) values.

- An improved and more accurate calculation of thermodynamical variables is implemented, both in the electromagnetic sector and the neutrino one. In particular, for the latter case we do not simply impose entropy conservation, but take into account entropy transfer during the $e^+ - e^-$ annihilation phase.

- We implemented an updated nuclear reaction network, obtained using new data and reduction techniques. Also, new reactions and new *types* of reactions (different number of nuclides in the initial and final states) are now included. The new code has been restructured so that it is easier to implement new reactions and that only fundamental nuclear data are needed as input. All derived quantities are calculated in the code. This is aimed at simplifying future updates.

- We improved the numerical resolution of the coupled BBN equations, by using a multistep method, belonging to the class of Backward Differentiation Formulas (instead of the traditional Runge-Kutta solver of the Kawano code which is a single step-method) implemented by a NAG routine. The default values of the accuracy parameters have been chosen to guarantee a good compromise between the accuracy goal and a reasonable running time. In particular the relative accuracy reached on ^{4}He mass fraction is of the order of 10^{-4}, thus keeping the numerical error below the level of theoretical uncertainties.

In Figure 2 we show the relative variation (in percent) of nuclear abundances computed with `PArthENoPE` and using the original Kawano code vs. baryon density, for the fiducial values of all the other parameters. To give an idea of the differences introduced by accounting for the major updates to the *physics* implemented in the code, in Table VII we report, for $\Omega_B h^2 = 0.022$ (i.e. consistent with the value singled out by the WMAP Collaboration [1]), the relative variation with respect to the Kawano code results of the theoretical prediction of abundances in three cases: 1) improved treatment of n-p weak rates, as presently in `PArthENoPE`, but original nuclear network as in Kawano code (first column); 2) improved treatment of n-p weak rates as presently in `PArthENoPE` and updated nuclear network as in Ref. [9] (second column); 3) `PArthENoPE` code, with improved calculation of thermodynamical variables, both in the electromagnetic sector and the neutrino one, and complete improvement of the nuclear network (third column). In summary, the `PArthENoPE` prediction for ^{4}He differs with respect to the original Kawano code by 0.7 %, mainly

Nuclide	weak rates (%)	nucl. rates (%)	Parthenope (%)
^{2}H	1.5	3.2	0.2
^{3}H	3.3	2.3	-0.7
^{3}He	0.1	-3.4	-1.1
^{4}He	0.4	0.4	0.7
^{6}Li	-2.7	12.2	2.8
^{7}Li	-1.8	2.9	1.3
^{7}Be	-2.0	2.5	1.6
^{9}Be	-0.1	200.0	200.0
^{10}B	1.3	-150.0	-153.8
^{11}C	200.0	146.0	153.8
^{12}C	0.4	0.5	-43.6

TABLE VII: The relative variation in percent of the theoretical predictions between `PArthENoPE` and the Kawano code, $\Delta X_i/\bar{X}_i \equiv 2(X_i^P - X_i^K)/(X_i^P + X_i^K)$, is shown for three cases (see text). The results are shown for $\Omega_B h^2 = 0.022$ and standard values for all other physical parameters.

due to the improved treatment of radiative corrections, finite temperature and finite nucleon mass corrections in neutron–proton weak rates. Actually, this value is larger than the theoretical accuracy of `PArthENoPE` on Y_p, which is of the order of 0.2%, see also [9]. On the other hand, our results are, for example, in very good agreement with [43], where all mentioned corrections to weak rates are included as discussed in details in [35]. Rescaling the value of neutron lifetime to the values $\tau_n = 886.7$ s adopted in [43] and using their fit for Y_p the agreement is at the 0.1% level. Concerning the other nuclides, the variation of the theoretical predictions with respect to the Kawano code reaches larger values, of the order of 3 % for ^{6}Li, at the 1% level for ^{7}Li and ^{7}Be, while it is very small for ^{2}H, as in this case the effects of improvements on weak rates treatment and updated nuclear rate network have different sign with respect to the one in plasma and neutrino treatment and almost cancel out accidentally. We notice that the introduction of new processes (reactions 98, 99, 100 of Table IV), see [22], and the update of those already considered in the Kawano code result in a large difference in the BBN theoretical prediction for metallicity, although probably insufficient to change the chemistry of primordial clouds. Finally, the reader may want to consider similar comparisons performed in the literature between updated versions of BBN codes used, e.g. in [44], [45] and the already quoted [43], and the results of the Kawano code presented in [21].

VI. CONCLUSIONS

In this paper we have described the general structure and features of `PArthENoPE` , a new numerical code which computes the theoretical abundances of nuclei produced during BBN, as function of several input cosmological parameters. This code has been recently made public and can be obtained at the URL http://parthenope.na.infn.it/. The code evaluates the abundances of 26 nuclide in the standard BBN scenario, as well as in extended models allowing for extra relativistic particles or neutrino chemical potential. We checked for a few fiducial cases that the results for the ^{4}He abundance agree very closely with those of Ref. [43], where the appropriate corrections [35] are applied to the original Wagoner/Kawano code [19, 20].

In view of the improved data coming from astrophysical observations, accurate tools providing theoretical predictions on cosmological observables are required to check the overall consistency of the picture of the evolution of the Universe, as well as for investigating and constraining new physics beyond the present framework of fundamental interactions.

Much effort has been put in the recent years by several groups in order to increase the level of accuracy of theoretical prediction on nuclide abundances, in particular by improving the estimate of the neutron to proton weak conversion rates and the nuclear network rates. The results of these studies, along with a to date analysis of experimental results on relevant nuclear reactions have been implemented in `PArthENoPE` , which hopefully will turn useful as an accurate tool for BBN-related studies.

Acknowledgments

In Naples, this work was supported in part by the PRIN04 “Fisica Astroparticellare e Cosmologia” and PRIN06 “Fisica Astroparticellare: neutrini ed universo primordiale” of the Italian MiUR. P.D.S. acknowledges support by the US Department of Energy and by NASA grant NAG5-10842.

APPENDIX A: DERIVATION OF THE PARTHENOPE SET OF EQUATIONS

We define $z \equiv m_e/T$, $x = m_e\, a$, $\bar{z} = x/z = aT = T/T_\nu$, $\hat{n}_B = m_e^{-3}\, n_B$ and introduce the following quantities:

$$\mathcal{N}(z) = \tfrac{1}{\bar{z}^4} \left(x \tfrac{d}{dx} \bar{\rho}_\nu \right) \Big|_{x=x(z)} \ , \ \bar{\rho}_\nu = a^4\, \rho_\nu = \left(\frac{x}{m_e} \right)^4 \rho_\nu \ , \tag{A1}$$

$$\rho = \rho_{e\gamma B} + \rho_\nu \ , \qquad \mathrm{p} = \mathrm{p}_{e\gamma B} + \mathrm{p}_\nu \ , \tag{A2}$$

$$\hat{\rho} = T^{-4}\, \rho = \left(\tfrac{z}{m_e} \right)^4 \rho \ , \qquad \hat{\mathrm{p}} = T^{-4}\, \mathrm{p} = \left(\frac{z}{m_e} \right)^4 \mathrm{p} \ . \tag{A3}$$

$$\tag{A4}$$

Starting from Eq.s (5) and (6),

$$\frac{\dot{n}_B}{n_B} = -\,3\, H \ , \tag{A5}$$

$$\dot{\rho} = -\,3\, H\ (\rho + \mathrm{p}) \ , \tag{A6}$$

and separating the neutrino contribution one gets

$$\dot{\rho}_{e\gamma B} + \dot{\rho}_\nu = -\,3\, H\, (\rho_{e\gamma B} + \mathrm{p}_{e\gamma B}) - \,4\, H\, \rho_\nu \ , \tag{A7}$$

where in (A7) we have used $\rho_\nu = 3\, \mathrm{p}_\nu$. From Eq. (A6) one gets the time derivative

$$\dot{\hat{\rho}} = \left(\frac{z}{m_e} \right)^4 \dot{\rho} + 4 \left(\frac{z}{m_e} \right)^3 \frac{\dot{z}}{m_e} \rho \ , \tag{A8}$$

and thus

$$\dot{\hat{\rho}}_{e\gamma B} = -\,3\, H\, (\hat{\rho}_{e\gamma B} + \hat{\mathrm{p}}_{e\gamma B}) + \,4\, \frac{\dot{z}}{z} \hat{\rho}_{e\gamma B} - \left(\frac{z}{m_e} \right)^4 (\dot{\rho_\nu} + \,4\, H\, \rho_\nu) \ . \tag{A9}$$

For the neutrino energy density one gets

$$\begin{aligned} \dot{\rho}_\nu = \frac{d\rho_\nu}{dx} \dot{x} = m_e \dot{a} \frac{d\rho_\nu}{dx} = H x \frac{d\rho_\nu}{dx} \ &= \ \left(\frac{m_e}{x} \right)^4 H \left[x \frac{d\bar{\rho}_\nu}{dx} - 4 \bar{\rho}_\nu \right] \ , \\ \dot{\rho}_\nu + \,4\, H\, \rho_\nu \ &= \ \left(\frac{m_e}{x} \right)^4 H x \frac{d\bar{\rho}_\nu}{dx} \ . \end{aligned} \tag{A10}$$

Hence substituting (A10) in (A9) we obtain

$$\dot{\hat{\rho}}_{e\gamma B} = 4\, \frac{\dot{z}}{z}\, \hat{\rho}_{e\gamma B} - \,3\, H\, (\hat{\rho}_{e\gamma B} + \hat{\mathrm{p}}_{e\gamma B}) - H\, \mathcal{N}(z) \ . \tag{A11}$$

On the other hand, the total time derivative of $\hat{\rho}_{e\gamma B}$ can be expressed via the partial derivatives with respect to z, ϕ_e and X_i ,

$$\dot{\hat{\rho}}_{e\gamma B} = \frac{\partial \hat{\rho}_{e\gamma B}}{\partial z}\, \dot{z} + \frac{\partial \hat{\rho}_{e\gamma B}}{\partial \phi_e}\, \dot{\phi}_e + \sum_i \frac{\partial \hat{\rho}_{e\gamma B}}{\partial X_i}\, \dot{X}_i = \left(\frac{\partial \hat{\rho}_{e\gamma B}}{\partial z} + \frac{\partial \hat{\rho}_{e\gamma B}}{\partial \phi_e}\, \frac{d\phi_e}{dz} + \sum_i \frac{\partial \hat{\rho}_{e\gamma B}}{\partial X_i}\, \frac{dX_i}{dz} \right) \dot{z} \ . \tag{A12}$$

Thus, equating the r.h.s of (A11) and (A12) after some rearrangement reads

$$\left(\frac{\partial \hat{\rho}_{e\gamma B}}{\partial z} - \frac{4}{z}\, \hat{\rho}_{e\gamma B} + \frac{\partial \hat{\rho}_{e\gamma B}}{\partial \phi_e}\, \frac{d\phi_e}{dz} + \sum_i \frac{\partial \hat{\rho}_{e\gamma B}}{\partial X_i}\, \frac{dX_i}{dz} \right) \dot{z} = -\,3\, z\, H\, (\hat{\rho}_{e\gamma B} + \hat{\mathrm{p}}_{e\gamma B}) - H\, \mathcal{N}(z) \ . \tag{A13}$$

Starting from (A5) and proceeding in the same way leads to

$$\left(\frac{\partial \hat{n}_B}{\partial z} + \frac{\partial \hat{n}_B}{\partial \phi_e}\, \frac{d\phi_e}{dz} + \sum_i \frac{\partial \hat{n}_B}{\partial X_i}\, \frac{dX_i}{dz} \right) \dot{z} = -\,3\, z\, H\, \hat{n}_B \ . \tag{A14}$$

Obtaining $\dot{z}$ from (A14) and substituting into (A13) we obtain

$$-3\,H\,\hat{n}_B\frac{\frac{\partial\hat{\rho}_{e\gamma B}}{\partial z}-\frac{4}{z}\hat{\rho}_{e\gamma B}+\frac{\partial\hat{\rho}_{e\gamma B}}{\partial\phi_e}\frac{d\phi_e}{dz}+\sum_i\frac{\partial\hat{\rho}_{e\gamma B}}{\partial X_i}\frac{dX_i}{dz}}{\frac{\partial\hat{n}_B}{\partial z}+\frac{\partial\hat{n}_B}{\partial\phi_e}\frac{d\phi_e}{dz}+\sum_i\frac{\partial\hat{n}_B}{\partial X_i}\frac{dX_i}{dz}}=-3\,z\,H\,(\hat{\rho}_{e\gamma B}+\hat{\mathrm{p}}_{e\gamma B})-H\,\mathcal{N}(z)\ . \tag{A15}$$

By using Eq. (8)

$$\hat{n}_B=\frac{\hat{L}(z,\phi_e)}{z^3\sum_i Z_i X_i}\ , \tag{A16}$$

one can express $\hat{n}_B$ and its derivatives as function of $\hat{L}(z,\phi_e)$ which is defined in (11). By solving Eq. (A15) with respect to $d\phi_e/dz$ one gets

$$\frac{d\phi_e}{dz}=\frac{1}{z}\frac{\hat{L}\,\kappa_1+\left(\hat{\rho}_{e\gamma B}+\hat{\mathrm{p}}_{e\gamma B}+\frac{\mathcal{N}(z)}{3}\right)\kappa_2}{\hat{L}\,\frac{\partial\hat{\rho}_e}{\partial\phi_e}-\frac{\partial\hat{L}}{\partial\phi_e}\left(\hat{\rho}_{e\gamma B}+\hat{\mathrm{p}}_{e\gamma B}+\frac{\mathcal{N}(z)}{3}\right)}\ , \tag{A17}$$

where

$$\kappa_1=4\,(\hat{\rho}_e+\hat{\rho}_\gamma)+\frac{3}{2}\,\hat{\mathrm{p}}_B-z\,\frac{\partial\hat{\rho}_e}{\partial z}-z\,\frac{\partial\hat{\rho}_\gamma}{\partial z}+\frac{1}{\hat{L}}\left(3\,\hat{L}-z\frac{\partial\hat{L}}{\partial z}\right)\hat{\rho}_B-\frac{z^2\,\hat{L}}{\sum_j Z_j\,X_j}\sum_i\left(\Delta\widehat{M}_i+\frac{3}{2\,z}\right)\widehat{\Gamma}_i\ , \tag{A18}$$

$$\kappa_2=z\,\frac{\partial\hat{L}}{\partial z}-3\,\hat{L}-z\,\hat{L}\,\frac{\sum_i Z_i\,\widehat{\Gamma}_i}{\sum_j Z_j\,X_j}\ . \tag{A19}$$

According to our notations, $\Delta\widehat{M}_i$ and $\widehat{M}_u$ stand for the i-th nuclide mass excess and the atomic mass unit, respectively, normalized to m_e, whereas $H\equiv m_e\,\widehat{H}$ and $\Gamma_i\equiv m_e\,\widehat{\Gamma}_i$. By substituting in (A14) the expression obtained for $d\phi_e/dz$ in (A17) we get

$$\dot{z}=-3\,H\frac{\frac{\partial\hat{n}_B}{\partial_{\phi_e}}\left(\hat{\rho}_{e\gamma B}+\hat{\mathrm{p}}_{e\gamma B}+\frac{\mathcal{N}(z)}{3}\right)-\hat{n}_B\,\frac{\partial\hat{\rho}_{e\gamma B}}{\partial\phi_e}}{\frac{\partial\hat{n}_B}{\partial_{\phi_e}}\left(\frac{\partial\hat{\rho}_{e\gamma B}}{\partial z}-\frac{4}{z}\hat{\rho}_{e\gamma B}+\sum_i\frac{\partial\hat{\rho}_{e\gamma B}}{\partial X_i}\frac{dX_i}{dz}\right)-\frac{\partial\hat{\rho}_{e\gamma B}}{\partial\phi_e}\left(\frac{\partial\hat{n}_B}{\partial z}+\sum_i\frac{\partial\hat{n}_B}{\partial X_i}\frac{dX_i}{dz}\right)}\ , \tag{A20}$$

namely

$$\frac{dt}{dz}=-\frac{\kappa_1\,\frac{\partial\hat{L}}{\partial\phi_e}+\kappa_2\,\frac{\partial\hat{\rho}_{e\gamma B}}{\partial\phi_e}}{3\,H\,\left[\hat{n}_B\frac{\partial\hat{\rho}_{e\gamma B}}{\partial\phi_e}-\frac{\partial\hat{n}_B}{\partial\phi_e}\left(\hat{\rho}_{e\gamma B}+\hat{\mathrm{p}}_{e\gamma B}+\frac{\mathcal{N}(z)}{3}\right)\right]}\ . \tag{A21}$$

The equations for the abundances (7) then become

$$\frac{dX_i}{dz}=\dot{X}_i\frac{dt}{dz}=-\frac{\widehat{\Gamma}_i}{3z\,\widehat{H}}\,\frac{\kappa_1\,\frac{\partial\hat{L}}{\partial\phi_e}+\kappa_2\,\frac{\partial\hat{\rho}_{e\gamma B}}{\partial\phi_e}}{\hat{L}\,\frac{\partial\hat{\rho}_e}{\partial\phi_e}-\frac{\partial\hat{L}}{\partial\phi_e}\left(\hat{\rho}_{e\gamma B}+\hat{\mathrm{p}}_{e\gamma B}+\frac{\mathcal{N}(z)}{3}\right)}\ . \tag{A22}$$

The solution of neutrino dynamics performed in [13–15] allows to compute the quantity

$$\mathcal{N}(z)=\left.\frac{1}{\bar{z}^4}\left(x\frac{d}{dx}\bar{\rho}_\nu\right)\right|_{x=x(z)}\ . \tag{A23}$$

Notice that $\mathcal{N}(z)$ would vanish for purely thermal neutrinos, and it is strictly related to the small entropy transfer to neutrinos during the e^+-e^- annihilation stage. In the code, $\mathcal{N}(z)$ is calculated by using the following fit, which is accurate to better than 0.1% in the relevant range:

$$\mathcal{N}(z)\ =\ \begin{cases}\exp\left(\sum_{l=1}^{13}n_l\ z^l\right) & z<4\quad,\\ 0 & z\geq 4\quad,\end{cases} \tag{A24}$$

with

$$
\begin{aligned}
n_0 &= -10.21703221236002 & n_1 &= 61.24438067531452 \\
n_2 &= -340.3323864212157 & n_3 &= 1057.2707914654834 \\
n_4 &= -2045.577491331372 & n_5 &= 2605.9087171012848 \\
n_6 &= -2266.1521815470196 & n_7 &= 1374.2623075963388 \\
n_8 &= -586.0618273295763 & n_9 &= 174.87532902234145 \\
n_{10} &= -35.715878215468045 & n_{11} &= 4.7538967685808755 \\
n_{12} &= -0.3713438862054167 & n_{13} &= 0.012908416591272199 \quad .
\end{aligned}
\tag{A25}
$$

APPENDIX B: COMMON VARIABLES USED IN PARTHENOPE

VARIABLE	DESCRIPTION	COMMON
AA(NNUC)	Nuclide atomic numbers, A_i	ANUM
FACTOR(NREC)	Multiplicative factor for the rate of reaction i-th	CHRATE
HCHRAT(NREC)	Type of changes adopted for reaction i-th	
NCHRAT	Number of reactions to be changed	
WCHRAT(NREC)	Reactions to be changed	
ALF	Fine structure constant, α	CONSTANTS
COEF(4)	Unity conversion factors	
GN	Newton constant, G_N, in MeV^{-2}	
ME	Electron mass, m_e	
MU	Atomic mass unit, M_u	
PI	π	
IFCN	Counter	COUNTS
IFCN1	Counter	
ISAVE1	Counter	
ISAVE2	Counter	
ISTEP	Counter	
DZ	Stepsize of the independent variable in the resolution of the nucleosynthesis equations	DELTAZ
DZ0	Initial value for DZ	
DM(0:NNUC)	Mass excesses in MeV, ΔM_i	DMASS
DMH(NNUC)	Adimensional mass excesses, $\Delta M_i/m_e$	DMASSH
PHI	Adimensional electron chemical potential, ϕ_e	ECHPOT
AG(NNUC,4)	Nuclear partition function coefficients	GPART
YY0(NNUC+1)	Initial values of electron chemical potential, ϕ_e, and nuclide abundances, X_i	INABUN
CMODE	Flag for the choice of the running mode	INPCARD
FOLLOW	Option for following the evolution on the screen (card mode)	
OVERW	Option for overwriting the output files (card mode)	
INC	Maximum value of the flag for the convergence of the matrix inversion	INVFLAGS
MBAD	Error flag for the matrix inversion	
LH0	Initial value for the adimensional electron/positron asymmetry, $\hat{L}$	INVPHI
Z0	Initial value for the evolution variable $z = m_e/T$ (=ZIN)	
AMAT(NNUC,NNUC)	Matrix involved in the linearization of the relation between $X_i(z+dz)$ and $X_i(z)$	LINCOEF
BVEC(NNUC)	Vector involved in the linearization of the relation between $X_i(z-dz)$ and $X_i(z)$ (contains X_i in reverse order)	
YX(NNUC)	$X_i(z)$ in reverse order	
YMIN	Numerical zero of nuclide abundances	MINABUN
DNNU	Number of extra effective neutrinos, ΔN_{eff}	MODPAR
DNNUXI	Contribution to the number of extra effective neutrinos from a non zero neutrino chemical potential, ΔN_{eff} of Eq. (25)	
ETAF	Final value of the baryon to photon density ratio, η_f	
IXIE	A positive integer fixing the electron neutrino chemical potential	
RHOLMBD	Energy density corresponding to a cosmological constant, ρ_Λ	
TAU	Value of neutron lifetime in seconds, τ_n	
XIE	Electron neutrino chemical potential, ξ (=XIE0)	
XIE0(NXIE)	Electron neutrino chemical potential, ξ	NCHPOT
INUC	Number of nuclides in the selected network	NETWRK
IREC	Number of reactions among nuclides in the selected network	
IXT(30)	Code of the nuclides whose evolution has to be followed (ixt(30)=control integer)	
NVXT	Number of nuclides whose evolution has to be followed	

VARIABLE	DESCRIPTION	COMMON
BYY(NNUC+1)	Text strings for the output	NSYMB
MN	Neutron mass, M_n	NUCMASS
MP	Proton mass, M_p	
NAMEFILE1	Name of the output file for the final values of the nuclide abundances	OUTFILES
NAMEFILE2	Name of the output file for the evolution of the nuclides whose evolution has to be followed	
NBH	Adimensional baryon number density, n_B/m_e^3	OUTVAR
THETAH	Adimensional Hubble function times 3, $3\widehat{H}$	
TXH	Neutrino to photon temperature ratio, T_X/T	
DZP	Previous iteration value of the step-size of the independent variable in the resolution of the nucleosynthesis equations	PREVVAL
SUMMYP	Value of the linear combination $\sum_i \left(\Delta\widehat{M}_i + \frac{3}{2\,z}\right) \widehat{\Gamma}_i$	
SUMZYP	Value of the linear combination $\sum_i \; Z_i \widehat{\Gamma}_i$	
ZP	Previous iteration value of the evolution variable $z = m_e/T$	
CFLAG	Flag for the input variable type in the card reading (card mode)	READINP
IKEY	Progressive argument key number in the card reading (card mode)	
ISTART	Starting point of the line in the card reading (card mode)	
DNCHRAT	Number of reactions to be added to the changed ones	
LINE	Line input from the card file (card mode)	
IFORM(NREC)	Reaction type (1-12)	RECPAR
NG(NREC)	Number of incoming nuclides of type TG	
NH(NREC)	Number of incoming nuclides of type TH	
NI(NREC)	Number of incoming nuclides of type TI	
NJ(NREC)	Number of incoming nuclides of type TJ	
NK(NREC)	Number of incoming nuclides of type TK	
NL(NREC)	Number of incoming nuclides of type TL	
Q9(NREC)	Energy released in reaction (in unit of 10^9 K)	
REV(NREC)	Reverse reaction coefficient	
TG(NREC)	Incoming nuclide type	
TH(NREC)	Outgoing nuclide type	
TI(NREC)	Incoming nuclide type	
TJ(NREC)	Incoming nuclide type	
TK(NREC)	Outgoing nuclide type	
TL(NREC)	Outgoing nuclide type	
RATEPAR(NREC,13)	Reaction parameter values (=IFORM+TI+...+NI+...)	RECPAR0
RSTRING(NREC)	Reaction text strings	RSTRINGS
LH	Function $\hat{L}$	THERMQ
LHPHI	Derivative of $\hat{L}$ with respect to ϕ_e	
LHZ	Derivative of $\hat{L}$ with respect to z	
NAUX	Neutrino auxiliary function, $\mathcal{N}(z)$	
PBH	Adimensional baryon pressure, $\hat{\mathrm{p}}_B$	
PEH	Adimensional electron pressure, $\hat{\mathrm{p}}_e$	
PGH	Adimensional gamma pressure, $\hat{\mathrm{p}}_\gamma$	
RHOBH	Adimensional baryon energy density, $\hat{\rho}_B$	
RHOEH	Adimensional electron energy density, $\hat{\rho}_e$	
RHOEHPHI	Derivative of $\hat{\rho}_e$ with respect to ϕ_e	
RHOEHZ	Derivative of $\hat{\rho}_e$ with respect to z	
RHOGH	Adimensional gamma energy density, $\hat{\rho}_\gamma$	
RHOGHZ	Derivative of $\hat{\rho}_\gamma$ with respect to z	
RHOH	Adimensional total energy density, $\hat{\rho}$	
GNUC(NNUC)	Nuclide spin degrees of freedom	SPINDF

VARIABLE	DESCRIPTION	COMMON
A(13)	Forward weak reaction best-fit parameters (non degenerate case)	WEAKRATE
B(10)	Reverse weak reaction best-fit parameters (non degenerate case)	
DA(12,NXIE)	Forward weak reaction best-fit parameters (degenerate case)	
DB(12,NXIE)	Reverse weak reaction best-fit parameters (degenerate case)	
QNP	Forward weak reaction best-fit exponent parameter	
QNP1	Forward weak reaction best-fit exponent parameter	
QPN	Reverse weak reaction best-fit exponent parameter	
QPN1	Reverse weak reaction best-fit exponent parameter	
ZZ(NNUC)	Nuclide atomic charges, Z_i	ZNUM

[1] D. N. Spergel *et al.* [WMAP Collaboration], astro-ph/0603449.
[2] B. Fields and S. Sarkar, arXiv:astro-ph/0601514.
[3] W. M. Yao *et al.* [Particle Data Group], Phys. Rev. D**66**, 010001 (2002).
[4] G. Steigman, Int. J. Mod. Phys. E **15**, 1 (2006) [arXiv:astro-ph/0511534].
[5] R.E. Lopez and M.S. Turner, Phys. Rev. D**59**, 103502 (1999) [astro-ph/9807279].
[6] S. Esposito *et al.*, Nucl. Phys. B**540**, 3 (1999) [astro-ph/9808196].
[7] S. Esposito *et al.*, Nucl. Phys. B**568**, 421 (2000) [astro-ph/9906232].
[8] S. Esposito *et al.*, JHEP **0009**, 038 (2000) [astro-ph/0005571].
[9] P. D. Serpico *et al.*, JCAP **0412**, 010 (2004) [astro-ph/0408076].
[10] N. Y. Gnedin and O. Y. Gnedin, Astrophys. J. **509**, 11 (1998) [astro-ph/9712199].
[11] A. D. Dolgov, S. H. Hansen, D. V. Semikoz, Nucl. Phys. B**543**, 269 (1999) [hep-ph/9805467].
[12] A. D. Dolgov, Phys. Rept. **370**, 333 (2002) [hep-ph/0202122].
[13] G. Mangano *et al.*, Phys. Lett. B**534**, 8 (2002) [astro-ph/0111408].
[14] G. Mangano *et al.*, Nucl. Phys. B**729**, 221 (2005) [hep-ph/0506164].
[15] G. Mangano *et al.*, Nucl. Phys. B**756**, 100 (2006) [hep-ph/0607267].
[16] R. H. Cyburt, Phys. Rev. D**70**, 023505 (2004) [astro-ph/0401091].
[17] A. Coc *et al.*, Astrophys. J. **600**,544 (2004) [astro-ph/0309480].
[18] C. Angulo *et al.*, Nucl. Phys. **A656**, 3 (1999), See the URL: http://pntpm.ulb.ac.be/nacre.htm.
[19] R.V. Wagoner *et al.*, Astrophys. J. **148**, 3 (1967); R.V. Wagoner, Astrophys. J. Suppl. **18**, 247 (1969); R.V. Wagoner, Astrophys. J. **179**, 343 (1973).
[20] L. Kawano, Let's go Early Universe *Preprint* Fermilab-Pub-92/04-A.
[21] M. S. Smith, L. H. Kawano and R. A. Malaney, Astrophys. J. Suppl. **85**, 219 (1993).
[22] F. Iocco *et al.*, Phys. Rev. D**75**, 087304 (2007) [astro-ph/0702090].
[23] D.S. Leonard *et al.*, Phys. Rev. C**73**, 045801 (2006) [nucl-ex/0601035].
[24] P. D. Serpico and G. G. Raffelt, Phys. Rev. D**71**, 127301 (2005) [astro-ph/0506162].
[25] Y. Z. Chu and M. Cirelli, Phys. Rev. D**74**, 085015 (2006) [astro-ph/0608206].
[26] A. Coc *et al.*, Phys. Rev. D**73**, 083525 (2006) [astro-ph/0601299].
[27] A. De Felice *et al.*, Phys. Rev. D**74**, 103005 (2006) [astro-ph/0510359].
[28] V. Barger *et al.*, Phys. Lett. B**569**, 123 (2003) [hep-ph/0306061].
[29] A. Cuoco *et al.*, Int. J. Mod. Phys. A**19**, 4431 (2004) [astro-ph/0307213].
[30] K. Jedamzik, Phys. Rev. D**70**, 063524 (2004) [astro-ph/0402344].
[31] P. D. Serpico and G. G. Raffelt, Phys. Rev. D**70**, 043526 (2004) [astro-ph/0403417].
[32] R. H. Cyburt *et al.*, Astropart. Phys. **23**, 313 (2005) [astro-ph/0408033].
[33] S. H. Hansen *et al.*, Phys. Rev. D**65**, 023511(2002) [astro-ph/0105385].
[34] G. Mangano *et al.*, JCAP **0703**, 006 (2007) [astro-ph/0612150].
[35] S. Sarkar, Rept. Prog. Phys. **59**, 1493 (1996) [hep-ph/9602260].
[36] A. D. Dolgov *et al.*, Nucl. Phys. B**632**, 363 (2002) [hep-ph/0201287].
[37] Y. Y. Y. Wong, Phys. Rev. D**66**, 025015 (2002) [hep-ph/0203180].
[38] K. N. Abazajian, J. F. Beacom and N. F. Bell, Phys. Rev. D**66**, 013008 (2002) [astro-ph/0203442].
[39] K. Freese, E. W. Kolb and M. S. Turner, Phys. Rev. D**27**, 1689 (1983).
[40] H. S. Kang and G. Steigman, Nucl. Phys. B**372**, 494 (1992).
[41] S. Esposito *et al.*, Nucl. Phys. B**590**, 539 (2000) [astro-ph/0005573].
[42] See the URL: http://www.nag.co.uk/numeric/fl/manual/html/FLlibrarymanual.asp
[43] G. Fiorentini, E. Lisi, S. Sarkar and F. L. Villante, Phys. Rev. D **58** (1998) 063506 [arXiv:astro-ph/9803177].
[44] R. H. Cyburt, B. D. Fields and K. A. Olive, New Astron. **6**, 215 (2001) [astro-ph/0102179].

[45] K. M. Nollett and S. Burles, Phys. Rev. D **61**, 123505 (2000) [astro-ph/0001440].